

Wave attenuation for dephasing and to measure conditional times

A. M. Jayannavar* and Colin Benjamin†

Institute of Physics, Sachivalaya Marg, Bhubaneswar 751 005, Orissa, India

(Dated: December 2, 2024)

Inelastic scattering induces dephasing in mesoscopic systems. An analysis of previous models to simulate inelastic scattering in such systems is presented and also a relatively new model based on wave attenuation is introduced. The problem of Aharonov-Bohm(AB) oscillations in conductance of a mesoscopic ring is studied. We have shown that conductance is symmetric under flux reversal and visibility of AB oscillations decay to zero as function of the incoherence parameter, signalling dephasing. Further wave attenuation is applied to a fundamental problem in quantum mechanics, i.e., the conditional(reflection/transmission) times spent in a given region of space by a quantum particle before scattering from that region.

PACS numbers: 72.10.-d, 73.23.-b, 05.60.Gg, 85.35.Ds, 03.65.-w, 03.65.Xp, 42.25.Bs

Keywords: Electron Transport, Dephasing, Sojourn times, Wave Attenuation

I. INTRODUCTION

We present a study of two different problems in mesoscopic physics which are of current interest namely, dephasing and the other conditional times. This work considers these two phenomena not from a microscopic point of view but through a phenomenological model which captures the essence of these quite well. This model is known as wave attenuation. It essentially involves damping the wave function in the region of interest, so as to derive essential physics. In the context of dephasing, we consider an Aharonov-Bohm interferometer, and show that the wave attenuation model is better than its counterpart the optical potential model used in this context. Also, in case of double heterostructures we employ this technique to clock the time a particle takes to traverse a local region of interest in the given system. Here also the wave attenuation model is more simpler to deal with than other models.

II. DEPHASING

The process of dephasing or decoherence leads to the diminishing of quantum effects or loss of quantum mechanical interference effects. Dephasing occurs due to interaction of an electron (interfering entity) with its environmental degrees of freedom (which are not measured in the interference experiment)[1, 2]. The AB oscillations are one of the prime examples for analyzing how quantum interference effects are affected by dephasing. These oscillations are similar to the fringes seen in an Young's double slit experiment apart from the presence of the magnetic flux. In the Young's double slit interferometer the intensity is given by $I = |\Psi|^2 = |\psi_1|^2 + |\psi_2|^2 + 2\Re(\psi_1^*\psi_2 e^{i\phi})$, the part $2\Re(\psi_1^*\psi_2 e^{i\phi})$ represents the interference term. Here ψ_1 and ψ_2 are the complex wave amplitudes across the upper and lower arms of the interferometer and ϕ is phase difference between these two wave amplitudes. If there would have been no phase relationship between the waves then the intensity will be $I = |\psi_1|^2 + |\psi_2|^2$. Complete dephasing is indicated by extinction of these interference terms. Thus, Dephasing can be defined as a phenomena by which quantum mechanical system behave as though they are described by classical probability theory.

A. Model's for dephasing

In absence of a complete microscopic theory as to how inelastic scattering affects dephasing, models are useful. There are different ways to model dephasing in mesoscopic systems. An interesting method is to attach a voltage probe[3] to the sample as in inset of Figure 1 (Buttiker's model). In this model, an electron captured by a voltage probe is re-injected back with an uncorrelated phase leading to irreversible loss of phase memory. This model has

*Electronic address: jayan@iopb.res.in

†Electronic address: colin@iopb.res.in

built in current conservation and Onsager's symmetry relations are obeyed but it does suffer from a major demerit in that it only describes localized dephasing.

The optical potential model provides another method of introducing dephasing in these mesoscopic samples. The optical potential was first introduced to explain the inelastic crossection in case neutron scattering. In this model a spatially uniform optical potential($-iV_i$) is added to the Hamiltonian[4], making it non-hermitian. This leads to removal of particles from phase coherent motion, while absorption is real in the case of photons there is no absorption for electrons. The absorption of electrons is reinterpreted[5] as scattering into other energy levels and therefore proper re-injection is necessary. Zohota and Ezawa[4] interpreted that the total transmission is defined after re-injection as the sum of two contributions one due to the coherent part and the other due to the incoherent part, i.e., $T_{tot} = T_{coh} + T_{incoh}$. The incoherent part is calculated as $T_{incoh} = \frac{T_r}{T_r + T_l} A$, herein T_r and T_l are the probabilities for right and left transmission from the region of inelastic scattering and A is the absorbed part which is given by $A = 1 - T_{coh} - R_{coh}$. This model unlike Buttiker's model describes dephasing that occurs throughout the system but still it has some major drawbacks in that it violates Onsager's two terminal symmetry relations[6] and in the limit of strong absorption leads to perfect reflection.

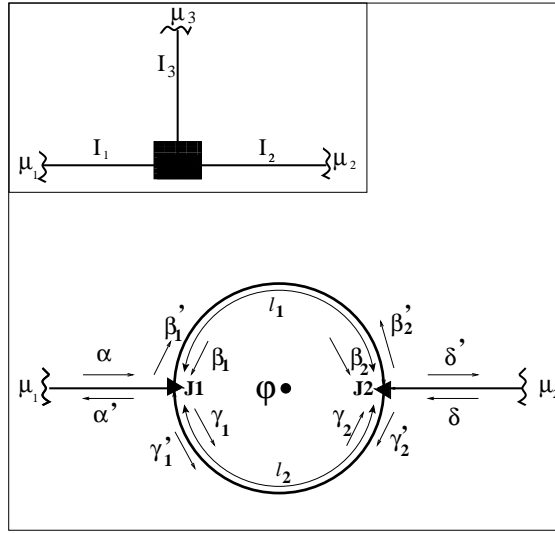


FIG. 1: Aharonov-Bohm ring geometry. Inset shows the three probe model.

Thus, there is need of a model which is free from the shortcomings of the above two models. Brouwer and Beenakker[7] have developed a simple method, by mapping the three probe Buttiker's method into a two terminal geometry, this is done by eliminating the transmission coefficients which explicitly depend on the third probe by means of unitarity of the S-matrix. They consider a three terminal geometry in which one of the probes is used as a voltage probe in absence of magnetic flux (see inset of Figure 1). A current $I = I_1 = -I_2$ flows from source to drain. In this model, a fictitious third lead connects the ring to a reservoir at chemical potential μ_3 in such a way that no current is drawn ($I_3 = 0$). The 3X3 S-matrix of the entire system can be written as-

$$S = \begin{pmatrix} r_{11} & t_{12} & t_{13} \\ t_{21} & r_{22} & t_{23} \\ t_{31} & t_{32} & r_{33} \end{pmatrix}$$

Application of the relations[3, 7, 8]- $I_p = \sum_q G_{pq}[\mu_p - \mu_q]$, $p = 1, 2, 3$ and $G_{pq} = (2e^2/h)T_{pq}$ yields the (dimensionless) two probe conductance $G = \frac{h}{2e^2} \frac{I}{\mu_1 - \mu_2}$,

$$G = T_{21} + \frac{T_{23}T_{31}}{T_{31} + T_{32}} \quad (1)$$

where $T_{pq} = T_{p \leftarrow q}$, is the transmission from q^{th} to p^{th} lead ($|t_{pq}|^2$), on elimination of the transmission coefficients in Eq. 1, which involve the voltage probe using the unitarity of the S - Matrix leads [7] to-

$$G = T_{21} + \frac{(1 - R_{11} - T_{21})(1 - R_{22} - T_{21})}{1 - R_{11} - T_{21} + 1 - R_{22} - T_{12}}. \quad (2)$$

Now all the above coefficients are built from the 2X2 S matrix-

$$S' = \begin{pmatrix} r_{11} & t_{12} \\ t_{21} & r_{22} \end{pmatrix}$$

which represents the S Matrix of the absorbing system (non-hermitian)[9]. Thus re-injection has been reformulated as in Eq. 2. The first term in Eq. 2 represents the conductance contribution from the phase coherent part. The second term accounts for electrons that are re-injected from the phase breaking reservoir, thereby ensuring particle conservation in the voltage probe model. Also, Eq. 2 restores Onsager's two terminal symmetry relation for the optical potential model.

B. Wave attenuation as a model for dephasing

In-spite of the fact that a major problem associated with the optical potential has been cured there still remains the problem that in the strong absorption limit it leads to perfect reflection and absorption without reflection(spurious scattering) is not possible [10, 11, 12]. To overcome this problem, we instead of making the Hamiltonian non-hermitian, add an exponential factor $e^{-\alpha l}$ to the S-Matrix of the system. This is the model of wave attenuation. This describes dephasing which occurs throughout the system and removes the short comings of the optical potential model.

The wave attenuation model is not new it has earlier been dealt with in the context of 1-D localization[10]. In the AB ring geometry considered here, wave attenuation is inserted by the factor $e^{-\alpha l_1}$ (or $e^{-\alpha l_2}$) in the complex free propagator amplitudes, every time we traverse[8] the upper (or lower) arms of the ring (see Figure 1). We have calculated the relevant transmission and reflection coefficients by using the S- matrix method along with the quantum wave guide theory for a single channel case. In this model, average absorption per unit length is given by 2α . With this method we show that the calculated conductance (G) in Eq. 2 is symmetric under the flux reversal as required. The visibility of the AB oscillations rapidly decay as a function of α , indicating dephasing. Hence forth we refer to α as an incoherence parameter. Increasing α corresponds to increasing dephasing processes in the system or increase in temperature.

In Figure 1, the length of the upper arm is l_1 and that of lower arm is l_2 . The total circumference of the loop is $L = l_1 + l_2$. The loop is connected to two current leads. The couplers (triangles) in Figure 1 which connect the leads and the loop are described by a scattering matrix S . The S matrix for the left coupler yields the amplitudes $O_1 = (\alpha', \beta'_1, \gamma'_1)$ emanating from the coupler in terms of the incident waves $I_1 = (\alpha, \beta_1, \gamma_1)$, and for the right coupler yields the amplitudes $O_2 = (\delta', \beta'_2, \gamma'_2)$ emanating from the coupler in terms of the incident waves $I_2 = (\delta, \beta_2, \gamma_2)$. The S-matrix for either of the couplers[13] is given by-

$$S = \begin{pmatrix} -(a+b) & \sqrt{\epsilon} & \sqrt{\epsilon} \\ \sqrt{\epsilon} & a & b \\ \sqrt{\epsilon} & b & a \end{pmatrix}$$

with $a = \frac{1}{2}(\sqrt{(1-2\epsilon)} - 1)$ and $b = \frac{1}{2}(\sqrt{(1-2\epsilon)} + 1)$. ϵ plays the role of a coupling parameter. The maximum coupling between reservoir and loop is $\epsilon = \frac{1}{2}$, and for $\epsilon = 0$, the coupler completely disconnects the loop from the reservoir.

The waves incident into the branches of the loop are related by the S Matrices for upper branch by-

$$\begin{pmatrix} \beta_1 \\ \beta_2 \end{pmatrix} = \begin{pmatrix} 0 & e^{ikl_1} e^{-\alpha l_1} e^{\frac{-i\theta l_1}{L}} \\ e^{ikl_1} e^{-\alpha l_1} e^{\frac{i\theta l_1}{L}} & 0 \end{pmatrix} \begin{pmatrix} \beta'_1 \\ \beta'_2 \end{pmatrix}$$

and for lower branch-

$$\begin{pmatrix} \gamma_1 \\ \gamma_2 \end{pmatrix} = \begin{pmatrix} 0 & e^{ikl_2} e^{-\alpha l_2} e^{\frac{i\theta l_2}{L}} \\ e^{ikl_2} e^{-\alpha l_2} e^{\frac{-i\theta l_2}{L}} & 0 \end{pmatrix} \begin{pmatrix} \gamma'_1 \\ \gamma'_2 \end{pmatrix}$$

These S matrices of course are not unitary $S(\alpha)S(\alpha)^\dagger \neq 1$ but they obey the relation $S(\alpha)S(-\alpha)^\dagger = 1$. The same relation is also obeyed by the S Matrix of the system in presence of imaginary potential. Here kl_1 and kl_2 are the phase increments of the wave function in absence of flux. $\frac{\theta l_1}{L}$ and $\frac{\theta l_2}{L}$ are the phase shifts due to flux in the upper and lower branches. Clearly, $\frac{\theta l_1}{L} + \frac{\theta l_2}{L} = \frac{2\pi\Phi}{\Phi_0}$, where Φ is the flux piercing the loop and Φ_0 is the flux quantum $\frac{\hbar c}{e}$. The transmission and reflection coefficients in Eq. 2 are given as follows- $T_{21} = |\frac{\delta'}{\alpha}|^2$, $R_{11} = |\frac{\alpha'}{\alpha}|^2$, $R_{22} = |\frac{\delta'}{\delta}|^2$, $T_{12} = |\frac{\alpha'}{\delta}|^2$ wherein $\delta', \delta, \alpha', \alpha$ are as depicted in Figure 1.

After calculating the required reflection and transmission coefficients we see that the coherent transmission T_{21} is not symmetric under the flux reversal however proper re-injection of carriers by Eq. 2 for the total conductance G plotted shows that the Onsager's symmetry relations are restored, i.e., G is symmetric under flux reversal. One can notice from this figure that amplitude of AB Oscillations decrease with increase in incoherence parameter α . All parameters used in the following figures are in their dimensionless form.

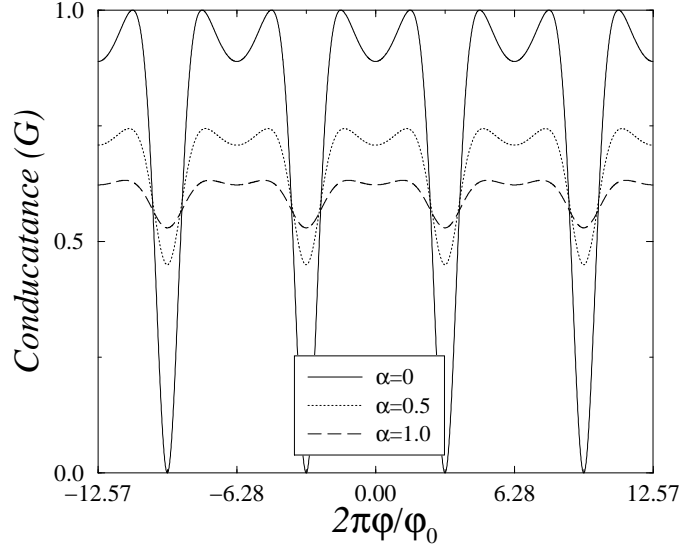


FIG. 2: Reduction of Aharonov-Bohm Oscillations in presence of incoherence parameter α . $kL = \pi$, $l_1/L = 0.75$, $l_2/L = 0.25$, and coupling $\epsilon = 0.5$.

In Fig. 3 we plot visibility (V) as a function of incoherence parameter α . Visibility is of course defined as

$$V = \frac{G_{max} - G_{min}}{G_{max} + G_{min}}. \quad (3)$$

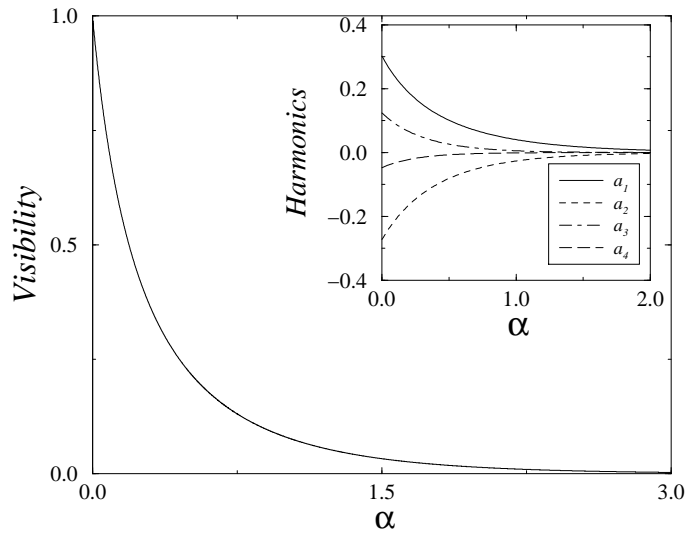


FIG. 3: Visibility for the same physical parameters as in Figure 2, coupling parameter $\epsilon = 0.5$. In the inset the harmonics have been plotted for the same physical and coupling parameters.

The plot shows that with increase in the value of the parameter α the visibility exponentially falls off, reaching a point where it becomes zero corresponding to the disappearance of quantum interference effects, i.e., total dephasing in

the system. In the inset of Figure 3 we have plotted the first few Fourier[14] harmonics a_n (wherein $n = 1$ to 4) of $G(\Phi)$ as a function of α . The harmonics are calculated from the formula- $a_n = \int_0^\pi G \cos(n\phi) d\phi$. The harmonics exponentially fall off with increasing α with exponent increasing as we go from 1 to 4. The n^{th} order harmonic corresponds to the contribution from electronic paths which encircle the flux n times. The harmonics can sometimes show non monotonic behavior depending on the physical parameters[15], however, the visibility is a monotonic function of the incoherence parameter α .

Thus we have seen that wave attenuation can be effective in modeling absorption induced dephasing in mesoscopic systems. In the next section we will see how this method is extended to measure the time a quantum particle takes to traverse a specified region of scattering.

III. TIME IN QUANTUM MECHANICS

One of the most important problem in quantum mechanics is to calculate the time spent by a particle in a given region of space before scattering from that region. The problem is essentially due to the fact that there is no hermitian operator to calculate this time in quantum mechanics[16, 17, 18]. The prospect of nanoscale electronic devices has in recent years brought new urgency to this problem as this is directly related to the maximum attainable speed of such devices. When it comes to tunneling time or time in general there is lot of ongoing controversy. In some formulations this time leads to a real quantity and in others to a complex quantity[19]. In certain cases tunneling time is considered to be ill-defined or quantum mechanics does not allow us to discuss this time[19, 20, 21]. Furthermore sometimes it is maintained that tunneling through a barrier takes zero time[22]. Recently, Anantha Ramakrishna and Kumar (AK)[23] have proposed the non unitary Optical potential as a clock to calculate the sojourn times without the clock affecting it. In this paper we examine another non-unitary clock, i.e., wave attenuation to calculate the conditional lengths, i.e., the total effective distance traveled by a particle in the region of interest. This conditional length on appropriate division by the speed of the particle in the region of interest will give us the conditional time.

The criteria, any result for the time spent by a quantum particle in a given region of scattering should satisfy are that-(1) It should be real, (2) It should add up for non overlapping regions, (3) It should be causally related to the interval of space, and (4) tend to the correct classical limits. It is shown explicitly by AK that all clock mechanisms involve spurious scattering or very clock mechanism affects the sojourn times to be clocked finitely even as the perturbation due to clock potential is infinitesimally small. All of these clocks involve spurious scattering as the perturbation due to clock mechanism couples to the Hamiltonian. This raises the question “Can quantum mechanical sojourn time be clocked with clock affecting it?”. In this paper we introduce such a method in which perturbation is not introduced in the Hamiltonian but in the S-Matrix of the system. In this case scattering is treated analogously with the Fabry-Perot interferometer. The scheme is illustrated in Figure 4.

A. Wave attenuation to measure conditional times

In the wave attenuation method[8, 10], we damp the wave function by adding an exponential factor ($e^{-\alpha l}$) every time we traverse the length of interest, here 2α represents the attenuation per unit length. This method is better than the optical potential model as it does not suffer from spurious scattering's[9, 11, 12]. The corrections introduced in case of Optical potential model to take care of spurious scattering's will become manifestly difficult when we calculate the traversal times for a superlattice involving numerous scatterer's. Thus our method of wave attenuation scores over the optical potential model. In the presence of wave attenuation a wave attenuates exponentially and thus the transmission (or reflection) coefficient becomes exponential with the length endured in presence of the attenuator and this acts as a natural counter for the sojourn lengths. Following the procedure of AK we calculate the traversal and reflection lengths and times in a given region of interest (in particular between two scatterer's as in Figure 4).

The amplitude for transmission and reflection can be calculated by summing[8] the different paths as in Figure 4. The scatterer S_1 in Figure 1 has as its elements r_1, r'_1, t_1 and t'_1 . r_1 is the reflection amplitude when a particle is reflected from the left side of the barrier while r'_1 is the reflection amplitude when a particle is reflected from the right side of the barrier. t_1 and t'_1 are the amplitudes for transmission when a particle is transmitted from left to right of the barrier and vice-versa. Similar assignments are done for the scatterer S_2 .

Thus for the amplitude of transmission we have- $t = t_1 t_2 e^{ik'l} e^{-\alpha l} + t_1 r'_1 r_2' t_2 e^{3ik'l} e^{-3\alpha l} + \dots$ which can be summed as

$$t = \frac{t_1 t_2 e^{ik'l} e^{-\alpha l}}{1 - r_2 r'_1 e^{2ik'l} e^{-2\alpha l}} \quad (4)$$

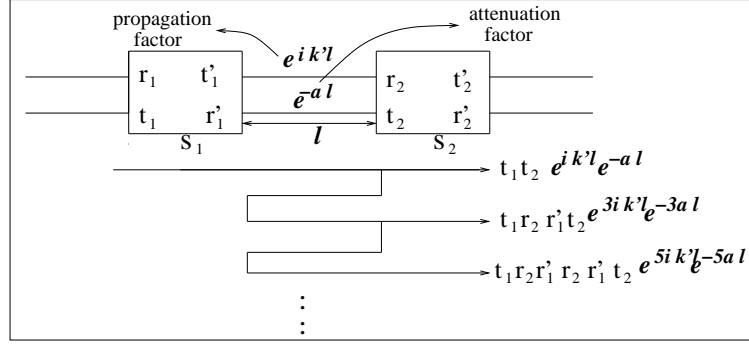


FIG. 4: Summing the different paths, S_1 and S_2 denote the two scatterer's. l is the distance between them. $e^{ik'l}$ and $e^{-\alpha l}$ denote the propagation and attenuation factors in the locality of interest.

and this is the transmission amplitude in presence of wave attenuation. Again for the case of reflection amplitude we have $r = r_1 + t_1 r_2 t'_1 e^{2ik'l} e^{-2\alpha l} + t_1 r_2 r'_1 r_2 t'_1 e^{4ik'l} e^{-4\alpha l} + t_1 r_2 r'_1 r_2 r'_1 r_2 t'_1 e^{6ik'l} e^{-6\alpha l} + \dots$, which leads to -

$$r = \frac{r_1 - ar_2 e^{2ik'l} e^{-2\alpha l}}{1 - r'_1 r_2 e^{2ik'l} e^{-2\alpha l}} \quad (5)$$

In Eq. 5, $a = r_1 r'_1 - t_1 t'_1$ is the determinant of the S-Matrix of the first barrier and as we are only dealing with unitary S-Matrices therefore the determinant is of unit modulus for all barriers. In these expressions k' is the wave vector in the region of interest. The transmission and reflection coefficients can be calculated by taking the square of the modulus of the expressions in Eq's. (4) and (5).

The traversal length for transmission and reflection are calculated as below[23]-

$$l^T = \lim_{2\alpha \rightarrow 0} -\frac{\partial(\ln |t|^2)}{\partial(2\alpha)} \quad (6)$$

and the reflection length in case of reflection is defined as-

$$l^R = \lim_{2\alpha \rightarrow 0} -\frac{\partial(\ln |r|^2)}{\partial(2\alpha)} \quad (7)$$

The traversal times for transmission or reflection times in case of reflection can be calculated from the formula $\tau^{R/T} = \frac{l^{R/T}}{\frac{\hbar k'}{m}}$ wherein as before $\frac{\hbar k'}{m}$ is the speed of propagation in the region of interest. For the case of the potential profile sketched in Figure 5, $k' = k$. From Eq's. (6) and (7) we can calculate the traversal length for transmission-

$$\frac{l^T}{l} = \frac{1 - |r'_1|^2 |r_2|^2}{1 - 2\Re(r'_1 r_2 e^{2ik'l}) + |r'_1|^2 |r_2|^2} \quad (8)$$

and for reflection-

$$\frac{l^R}{l} = \frac{l^T}{l} + \frac{|r_2|^2 - |r_1|^2}{|r_1|^2 - 2\Re(r_1^* r_2 a e^{2ik'l}) + |r_2|^2} \quad (9)$$

Here \Re represents real part of the quantity in brackets. In the above two equations the traversal and reflection lengths have been normalized with respect to the length l of the locality of interest, which is the well region of the potential profile of Figure 5. Throughout the discussion the quantities are expressed in their dimensionless form.

We consider the case of two rectangular barriers as shown in Figure 5 separated by a distance l . The energies, potentials and the lengths are all in their dimensionless form.

The S-Matrices for the double heterostructure are given as-

$$S_j = \begin{pmatrix} r_j & t'_j \\ t_j & r'_j \end{pmatrix} = \begin{pmatrix} \frac{-i\epsilon_{j+} \sinh K_j a_j}{2 \cosh K_j a_j - i\epsilon_{j-} \sinh K_j a_j} & \frac{1}{2 \cosh K_j a_j - i\epsilon_{j-} \sinh K_j a_j} \\ \frac{2e^{-ika_j}}{2 \cosh K_j a_j - i\epsilon_{j-} \sinh K_j a_j} & \frac{-e^{-2ika_j} i\epsilon_{j+} \sinh K_j a_j}{2 \cosh K_j a_j - i\epsilon_{j-} \sinh K_j a_j} \end{pmatrix}$$

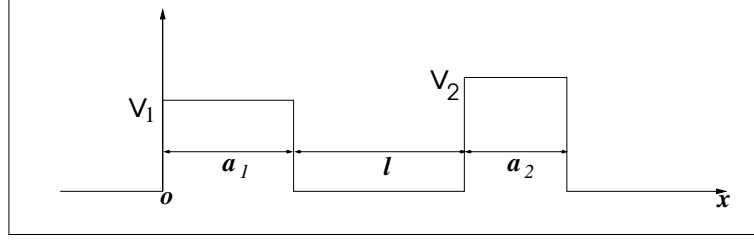


FIG. 5: The double heterostructure. Barrier's are denoted by length a_j 's, height V_j 's and $j = 1, 2$. The length of the well is l .

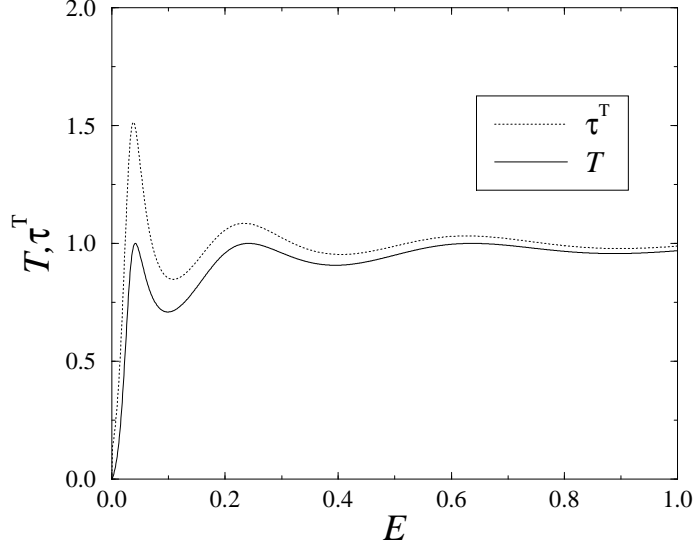


FIG. 6: T and τ^T for a symmetric double heterostructure . $l = 10.0$, $V_1 = V_2 = 1.0$ and $a_1 = a_2 = 0.2$.

wherein $K_j = \sqrt{\frac{2m(V_j - E)}{\hbar^2}}$, $k = \sqrt{\frac{2mE}{\hbar^2}}$ and $\epsilon_{j\pm} = \frac{k}{K_j} \pm \frac{K_j}{k}$. Herein, $j=1,2$.

In Figure 6 we plot the Transmission coefficient and the normalized times τ^T ($=\tau^R$) for a symmetrical double barrier $V = V_1 = V_2$. These times are those required by a quantum particle to traverse or reflect from the well of the double heterostructure. We have normalized these times by the time taken by a particle to traverse the length l , i.e., $\frac{ml}{\hbar k}$ without the potential profile as in Figure 5. From Eq. 8, it is clear that transmission time is always positive. Moreover, we can readily show from our treatment that local times spent by the particle in non-overlapping regions are additive. As expected the traversal times are larger near the resonances. In case of non-symmetrical structures one obtains negative reflection times (which should not be surprising) in some parameter region but traversal times are positive for both symmetrical as well as non-symmetrical structures. It can be argued[23] that this is because in case of reflection there is a partial wave corresponding to prompt reflection r_1 that never samples the region of interest, and also this prompt part leads to self interference delays which cause the sojourn time τ^R to become negative for some values of the parameters. If one removes this prompt part, i.e., $r_{np} = r - r_1$, and we re-calculate the sojourn time $\tau^{R_{np}}$ with this prompt part removed we find it to be positive and given by $\tau^{R_{np}} = \tau^T + 1$, as τ^T is positive. In the case of non-symmetrical structures τ^T is independent of the fact that a particle is incident from the left or the right, but τ^R depends on the direction of the incident particle. There is also a remarkable assertion found in the literature[17] concerning the measurement of the time of transmission or reflection, which is $\tau^D = T\tau^T + R\tau^R$. Herein τ^T and τ^R are as given above while the dwell time $\tau^D = \frac{1}{v} \int_0^l |\psi|^2 dx$. ψ is the wavefunction in the locality of interest and v is the speed of the particle in the region of interest. We have verified explicitly after calculation that this equivalence does not hold [16, 24]. Our method can also be readily extended to calculation of traversal time of tunneling (for case of a single barrier). Results are in agreement with recent calculations[23].

IV. CONCLUSION

In conclusion, we have shown that wave attenuation is much better in modeling dephasing due to absorption than it's counterpart the optical potential. Further when we extend this method to calculate the conditional sojourn times we find here also wave attenuation is easier to deal with than optical potential.

[1] Y. Imry, *Introduction to Mesoscopic Physics* (Oxford University Press, New York, 1997).

[2] Florian Marquardt, *An Introduction to the basics of dephasing* (<http://iff.physik.unibas.ch/~florian/dephasing/dephasing.html>).

[3] M. Buttiker, Phys. Rev. **B33**, 3020 (1986); IBM J. Res. Dev. **32**, 63 (1988).

[4] Y. Zohta and H. Ezawa, J. Appl. Phys. **72**, 3584 (1992).

[5] Hu Yuming, J. Phys. **C21**, L23 (1988).

[6] T. P. Pareek, Sandeep K. Joshi, and A. M. Jayannavar, Phys. Rev. **B57**, 8809 (1998);

[7] P. W. Brouwer and C. W. J. Beenakker, Phys. Rev. **B55**, 4695 (1997); P. W. Brouwer, Ph.D. thesis, Insttuut-Lorentz, University of Leiden, The Netherlands, 1997.

[8] S. Datta, *Electron Transport in mesoscopic systems* (Cambridge University press, Cambridge, 1995).

[9] Colin Benjamin and A. M. Jayannavar, Phys. Rev. **B65**, April 15 (2002), in press; preprint cond-mat/0112153.

[10] Sandeep K. Joshi, D. Sahoo and A. M. Jayannavar, Phys. Rev. **B62**, 880 (2000); P. Pradhan, preprint cond-mat/9807312.

[11] A. M. Jayannavar, Phys. Rev. **B49**, 14718 (1994); A. K. Gupta and A. M. Jayannavar, Phys. Rev. **B52**, 4156 (1995).

[12] A. Rubio and N. Kumar, Phys. Rev. **B47**, 2420 (1993).

[13] M. Buttiker, Y. Imry and M. Ya. Azbel, Phys. Rev. **A30**, 1982 (1984).

[14] J. B. Xia, Phys. Rev. **B45**, 3593 (1992).

[15] S. K. Joshi, D. Sahoo and A. M. Jayannavar, Phys. Rev. **B64**, 075320 (2001).

[16] R. Landauer and Th. Martin, Rev. of Mod. Phys. **66**, 217 (1994).

[17] E. Hauge and J. A. Stovneng, Rev. of Mod. Phys. **61**, 917 (1989).

[18] V. . Gasparian, M. Ortuno, G. Schon and U. Simon, *Tunneling time in Nanostructures* (<http://bohr.fcu.um.es/papers/1999/gasparian.pdf>).

[19] D. Sokolovski and L. M. Baskin, Phys. Rev. **A36**, 4604 (1987).

[20] N. Yamada, Phys. Rev. Lett. **83**, 3350 (1999).

[21] A. Steinberg, Phys. Rev. Lett. **74**, 2405 (1995).

[22] E. O. Kane, in *Tunneling Phenomena in Solids*, edited by E. Burstein and S. Lundquist (Plenum, New York), p.1 (1969).

[23] S. Anantha Ramakrishna and N. Kumar, preprint cond-mat/0009269; S. Anantha Ramakrishna, Ph. D Thesis, Raman Research Institute, Bangalore, India (2001).

[24] Colin Benjamin and A. M. Jayannavar, Solid State Comm. (2002), in press; preprint cond-mat/0112499.